Title

High-Throughput Profiling of Nanoparticle–Protein Interactions by Fluorescamine Labeling

Journal

Analytical Chemistry, 87(4)

ISSN

0003-2700

Authors

Ashby, Jonathan
Duan, Yaokai
Ligans, Erik
et al.

Publication Date

2015-02-17

DOI

10.1021/ac5036814

Peer reviewed

High-throughput profiling of nanoparticle-protein interactions by fluorescamine labeling

Jonathan Ashby[1]*,Yaokai Duan*[1]*, Erik Ligans*[2+]*, Michael Tamsi*[1.2+]*, Wenwan Zhong*[1,*]

[1]Department of Chemistry, [2]Department of Biology, University of California, Riverside

Keywords: Fluorescamine, nanoparticle-protein interactions, nanoparticle physical parameters

Abstract

A rapid, high throughput fluorescence assay was designed to screen interactions between proteins and nanoparticles. The assay employs fluorescamine, a primary-amine specific fluorogenic dye, to label proteins. Since fluorescamine could specifically target the surface amines on proteins, a conformational change of the protein upon interaction with nanoparticles will result in a change in fluorescence. In the present study, the assay was applied to test the interactions between a selection of proteins and nanoparticles made of polystyrene, silica, or iron oxide. The particles were also different in their hydrodynamic diameter, synthesis procedure, or surface modification. Significant labeling differences were detected when the same protein incubated with different particles. Principal component analysis (PCA) on the collected fluorescence profiles revealed clear grouping effects of the particles based on their properties. The results prove that fluorescamine labeling is capable of detecting protein-nanoparticle interactions, and the resulting fluorescence profile is sensitive to differences in nanoparticle physical properties. The assay can be carried out in a high-throughput manner, and is rapid with low operation cost. Thus, it is well suited for evaluating interactions between a larger number of proteins and nanoparticles. Such assessment can help to improve our understanding on the molecular basis that governs the biological behaviors of nanomaterials. It will also be useful for initial examination of the bioactivity and reproducibility of nanomaterials employed in biomedical fields.

While promising nanomaterial-based biosensors, imaging probes, drug carriers, *et cetera*, have been developed, implementation of these materials in biomedical fields is still hindered by the lack of a thorough understanding about the implications of nanomaterials on biological systems.[1] It has been established that the behaviors of nanomaterials in biosystems is strongly influenced by their interaction with proteins.[2,3] The protein interaction behaviors of nanomaterials could be indicative of their biological activity.[4] Nanomaterials can be produced with distinct or subtle differences in chemical composition, size, shape, surface modification, *et cetera*.[5-7] Proteins are highly diverse in their properties as well. Changes in properties of both proteins and particles can strongly influence interactions between the two, making it necessary to conduct such studies on large sample sets with a fast and high-throughput assessment method.

Nanoparticle-protein interactions have been evaluated by separation[8] and spectroscopic techniques,[9] but problems exist with these methods, including requirements for target immobilization, multi-step sample processing, or protein/particle modification. Alternatively, screening of protein adsorption on nanomaterials in biological matrices has been achieved using proteomic techniques;[3] and the adsorption profile was found to be dependent on the properties of the nanomaterial used.[10] Proteins undergo structural changes upon interacting with nanomaterials,[11] and the changes could be strongly influenced by the properties of nanomaterials; such as surface curvature,[5,12] chemical structure of surface coating,[7,13] and core material.[14] Protein structural changes during interaction with nanomaterials can be assessed by circular dichroism,[15] enzymatic activity measurement,[16] or dynamic light scattering;[17] but they are time consuming, tedious, and low throughput.

Herein, we developed a high-throughput assay for rapid screening of the interactions between proteins and nanomaterials. The assay relies on simple yet rapid protein labeling via a

fluorogenic dye, fluorescamine, which is activated upon reaction with a primary amine.[18] This property has been employed to label peptides and small molecules prior to chromatographic analysis, quantifying proteins in a sample[19] as well as counting amine sites on nanomaterial surfaces.[20,21] In the present study, we tested whether fluorescamine labeling could be used to detect protein-nanoparticle interaction, and how the resulting fluorescence profile was related to the properties of nanomaterials.

Materials and Methods

R*eagents used in the study.* Fluorescamine was purchased from either Life Technologies (Carlsbad, CA) or Sigma-Aldrich (St. Louis, MO). Solid HEPES was purchased from CalBioChem (EMD Millipore, Darmstadt, Germany). Sodium phosphate monobasic monohydrate, anhydrous sodium phosphate dibasic, sodium chloride, sodium tetraborate, tris base, sodium hydroxide, hydrochloric acid, ethanol, dimethyl formamide (DMF), dithiothreitol, iodoacetamide and glycine were all purchased from Thermo Fisher Scientific (Waltham, MA). All proteins were obtained from Sigma-Aldrich.

Nanomaterials investigated. Polystyrene (PS) nanoparticles with a carboxylated surface and core diameter of 42, 48 or 85 nm were purchased from Polysciences (Warrington, PA). Silica particles were synthesized in-house (synthesis in Supporting Methods) with varying degrees of surface carboxylation. Iron oxide nanoparticles (IONPs) with a 10-nm core diameter and coated by either an amphiphilic polymer (10-AMP-1, 10-AMP-2) or polyethylene glycol (10-PEG) were purchased from Ocean Nanotech (Springdale, AR).

Capability of fluorescamine in labeling amines on protein surface. Apha-1-antitrypsin, succinyl concanavalin A, transferrin and human serum albumin were incubated in 50% ethanol

(EtOH) aqueous solution to induce extreme conformational changes. Alcohol denaturation was conducted for 30 minutes at 37˚C. After denaturation, the protein was incubated with fluorescamine (final protein and dye concentrations were 100 nM and 1 mM, respectively) for 10 minutes before fluorescence detection on the Victor II plate reader. As a control, proteins were treated under identical conditions with the 50% EtOH replaced by the 10 mM phosphate buffer (pH 8.0 with 50 mM NaCl). To confirm that the fluorescence increase was due to protein conformational change, circular dichroism (CD) was conducted on two selected proteins to assay changes in secondary structure. CD spectra were collected on a Jasco J-815 spectrometer (details in Supporting Methods), and the secondary structure determined by the method outlined in Raussens *et al*.[22]

On-plate fluorescamine assays for determining changes in the physicochemical properties of nanoparticles. The mixture of 400 nM protein and 40 nM particles were incubated at 37 °C for 2 hrs in 10 mM phosphate (pH 8.0, 50 mM NaCl). The final volume for the mixture was 100 µL. For each protein-particle pair, two controls were included. One contained only the protein; and the other had only the particles in the buffer. After incubation, the sample was transferred to a 96-well plate. Five µL fluorescamine was added to each well (final concentration1 mM) and reacted for 10 min at room temperature. The plate was analyzed using the Victor II plate reader. Experiments were conducted in triplicate.

Afterward, the fluorescence intensity for each protein-particle pair was normalized to the particle-free signal, and the normalized values for all pairs were subject to principal components analysis (PCA). The scores plot was prepared using the first two principal components to show the grouping effect of nanoparticles. The loadings plot was used to determine the relative contribution of each protein to the particle's location on the scores plot.

Fluorescamine assay coupled with on-filter digestion for non-transparent particles. In an Eppendorf tube, 400 nM of HSA, transferrin or thyroglobin and 40 nM of the IONPs were incubated in 10 mM phosphate (pH 8.0, 50 mM NaCl) for 2 hours at 37 °C. After incubation, the samples were treated with 1 mM fluorescamine for ten minutes at room temperature. Samples were then quenched with 10 mM tris buffer, and transferred to a 30 kDa Amicon filter. The protein samples were digested on-filter using a modified filter-aided sample preparation (FASP) protocol (Supporting Information).[23] The post-digestion flow-through was then transferred to a 96-well plate and analyzed on the Victor II plate reader. Experiments were conducted in duplicate or triplicate.

Results and Discussion

Nanoparticles and proteins used in the study. All nanoparticles chosen for this study are listed in Table 1. The carboxylated PS and silica particles, representing optically transparent nanomaterials, were used in the on-plate assay. Two of the PS samples were from different batches of the same product, with an average diameter of 45 nm. The third PS sample had a larger diameter of 85 nm. The silica particles, fabricated by a modified Stöber synthesis,[24] also functionalized with carboxyl groups. Particles were aminated for various times prior to the 24-hour carboxylation process. DLS and zeta-potential measurements indicated that all silica particles had similar hydrodynamic diameters of 85-95 nm with small differences in surface charge density. These transparent particles vary in core material, size, or synthetic pathway, and in this study, their interactions with proteins having different Mw and pI values were explored by fluorescamine labeling using the simple on-plate assay format.

The IONPs were chosen as a non-transparent case to show the applicability of this assay over a wider range of nanomaterials. Such particles strongly absorb the fluorescent signal from the reacted fluorescamine, and thus were not suitable for the on-plate assay. Instead, the proteins were digested after particle interaction and fluorescamine labeling, and the peptides were analyzed. All IONPs had a similar core diameter of 10 nm, but were different in their surface coating: they were covered by either PEG or AMP.

As proof of principle, succinyl concanavalin A (ConA), alpha-1-antitrypsin (A1AT), serum albumin (HSA), transferrin, haptoglobin, and apolipoprotein A1 (APOA1) were employed. Such proteins have well-known and well-characterized tertiary structures in the RSCB Protein Data Bank. The structures helped to calculate the numbers of surface-accessible amines of these proteins in their native structures, for assessment of fluorescamine's capability in targeting such amines. Screening of protein interaction on all of the selected nanoparticles was done on proteins with different size/Mw, isoelectric point, and hydrophobicity (Table S1): cytochrome C (cyt C), hemoglobin, catalase, HSA, transferrin, fibrinogen and thyroglobulin. Protein hydrophobicity was represented by the grand average of hydropathy (GRAVY) scores calculated using ProtParam, a tool available in the SIB ExPASy Bioinformatics Resources Portal.[25] The selected proteins covered a wide range of Mw (from 11.5 to 300 kDa), pI (from 5.2 to 9.5), hydrophobicity (GRAVY score from -0.004 to -0.885), and number of primary amines (from 17 to 255).

Inclusion of proteins and nanoparticles possessing diverse properties is necessary in high throughput screening of protein-nanoparticles, in order to reveal the key parameters that influence protein-nanoparticle interaction.

Optimization of fluorescamine reactivity. In order to capture changes in protein conformation during interaction with nanomaterials, the labeling reaction must be rapid and efficient. We studied the reaction of fluorescamine with glycine under different conditions (Supplemental Methods). The choice of buffer, as well as buffer pH and salt concentration, were optimized for maximum reactivity (slope of the fluorescence vs. glycine concentration plot) and a low limit of detection (LOD). Of the three buffers chosen, phosphate yielded the highest reactivity compared to HEPES and MES at the same pH of 7.5 (Table S2). Investigation of reactivity in 10 mM phosphate at pH 6.0, 7.0, 7.5, and 8.0, showed the steepest fluorescence increase at the higher pH. More primary amines will be deprotonated under basic pH, allowing for a more rapid and complete reaction with fluorescamine. NaCl concentrations from 0, to 50, 100 and 150 mM were tested, with little change in reactivity observed. Since a large amount of salt could cause nanoparticle aggregation due to reduction in electrostatic repulsion between particles, we used 50 mM NaCl to maintain protein's secondary structure.[26] In 10 mM phosphate at pH 8.0 with 50 mM NaCl, the resulting fluorescence reached a plateau at 60 min, with 85% of the maximum value achieved within five minutes (Figure S1). This buffer was used in all of the following studies, and the reaction time was fixed at ten minutes to permit adequate labeling.

Capability of fluorescamine in targeting the surface amines of protein. In addition to reacting with primary amines, fluorescamine is also hydrolyzed in a basic, aqueous solution, yielding a non-fluorescent product.[21] The short life time in aqueous environment facilitates it to only react with the most-available amines in a protein before being hydrolyzed. To determine whether fluorescamine possessed specificity towards surface amines on a protein, four proteins – ConA, A1AT, HSA and transferrin –were incubated under harsh denaturation conditions (50% ethanol) before fluorescamine was added to react with the surface amines. After the ethanol treatment

fluorescence was found to increase by 100-300% (Figure 1) in all proteins except for ConA. No fluorescamine labeling was detected for this protein in its native or denatured form, which could be due to lack of surface amines on this protein. Protein structural changes caused by denaturation were confirmed by circular dichroism (CD) measurements on HSA and transferrin. The CD spectra were processed as in our previous report[43] to calculate the percentage of alpha helix, beta sheet, and random coil in the overall protein structure (Supporting Information Figure S2). In agreement with the fluorescamine labeling results, the percentage of alpha helix in HSA incubated in 50% ethanol was significantly lower than that in the phosphate buffer (Fig. S2A), while the percent of both the beta sheet and random coil increased. For transferrin, more alpha helix was generated in 50% ethanol, accompanied with some loss of random coil (Fig. S2B).

To further confirm its selectivity towards surface amines, fluorescamine was incubated with A1AT, APOA1, haptoglobin, HSA, and transferrin, respectively, in the phosphate buffer. Using a calibration curve made from glycine, the number of fluorescamine labeling events per protein molecule was calculated by the following equation:

$$\#\text{of labeling events} = \frac{\frac{(F_{protein})}{(Mol_{protein})}}{\left(\frac{F_{glycine}}{Mol_{glycine}}\right)}$$

where F is the raw fluorescence of either the protein sample or the glycine standard. This value was compared to the total numbers of Lys/Arg in each protein (as determined from the protein sequence) as well as the solvent-accessible surface amine residues, which were determined through GETAREA (Table 2), an online application provided by the University of Texas Medical Branch.[27] Table 2 shows that, for most proteins, there was good agreement between the experimentally determined and theoretically calculated number of surface amines, giving strong

support to the surface-specificity of fluorescamine. The only exception was transferrin: the number of detected amines was larger than the number of solvent accessible amines. This can be attributed to the 3D structure used. Only dimeric transferrin complexes are found in the RSCB, which would lead to some surface amines being buried at the protein interface and no longer being recognized as solvent accessible by GETAREA. Due to fluorescamine's rapid reactivity and inactivation in water, it cannot enter the core of the protein before being hydrolyzed. As a result, fluorescamine can only target solvent accessible (surface) amines. This result also proves that, fluorescamine labeling by itself would not disturb protein structure. Otherwise, a significantly higher number of labeling events than the calculated number of surface amines would be detected in all of the tested proteins due to exposure of the buried lysine and arginine residues.

Fluorescamine assay for revealing interaction between proteins and nanoparticles. Specific labeling of a protein's surface by fluorescamine could be useful for detection of interaction between proteins and nanoparticles. Once the protein is adsorbed onto the nanoparticle, the number of surface amines would change due to disturbances in the protein's tertiary structure and formation of the binding interface, altering the labeling result. We examined the interaction of HSA and transferrin with the 42-nm carboxylated PS particles by fluorescamine labeling. Compared to the protein itself, the resulting fluorescence upon interaction with the nanoparticles increased by 1.5 and 3 fold for HSA and transferrin, respectively (Figure 2A, particle labeled as PS-1). CD measurement confirmed that interaction with the PS particles significantly increased the content of alpha helix and slightly reduced random coils in transferrin (Fig. S2B). Such conformational changes in protein structure may have exposed more amines for fluorescamine to label. Agreeing with the fluorescamine result, the degree of conformational changes in HSA

detected by CD was much lower than that in transferrin when adsorbed by the PS particles: no noticeable change was detected by CD in HSA (Fig. S2A). A large protein-to-particle molar ratio of 100:1 was used in CD measurement for reduction of the background UV absorbance from the nanoparticles. The number of HSA adsorbed by the nanoparticles was too small among the bulk population of the HSA molecules to induce sufficient change detectible by CD.

Relationship between fluorescence profile and particle properties. We further explored the relationship between protein labeling and nanoparticle properties. Interactions between various PS and silica nanoparticles and a group of proteins were examined using the fluorescamine assay. Each of the six different nanoparticles incubated with seven individual proteins were screened per experiment, plus the corresponding particle-only and protein-only controls. A 96-well plate was used to simultaneously test such a high number of samples. All fluorescence signals of the protein-particle mixtures were normalized to that of the protein-only blank and listed in Table S3. The fluorescence was found to increase for most proteins upon binding to the nanoparticles, reflecting the exposure of more surface amines due to conformational change in protein structure. The particles could react with fluorescamine, but the resulting signal was negligible compared to that observed in the protein-particle incubations.

To interpret the effects of particle properties on protein interactions, we focused on nanoparticles differing in one property aspect and compared their fluorescence profiles. Figure 2A compared the average normalized fluorescence observed from proteins when incubated with the carboxylated PS particles of different diameters. Fluorescence profile comparison of the silica particles with varying amination durations before the carboxylation step during synthesis was shown in Figure 2B. For both the PS and silica particle groups, larger normalized fluorescence were obtained with cyt C and hemoglobin, the two proteins with higher pIs than

others. Hemoglobin is neutral and cyt C is slightly positively charged at pH 8.0, which could induce stronger electrostatic interaction with the negatively charged carboxylated particles than the remaining, five acidic proteins. While all proteins showed significant changes in fluorescamine labeling when interacting with the PS particles, the three types of silica particles did not cause noticeable fluorescence increase in most of the tested proteins, except for the largest one, thyroglobulin.

To summarize the overall variations in fluorescamine labeling on different protein-nanoparticle pairs, the normalized fluorescence dataset shown in Table S3 was subjected to principal components analysis (PCA). The free data mining software TANAGRA, developed by Ricco Rakotomalala,[28] was used and the PCA results were exported to Origin and plotted. During PCA, each repetition (an average of three replicates on plate) of the same protein-nanoparticle pair was treated as one individual observation; and the proteins were viewed as variables. The resulting scores plot was displayed in Figure 3. Interestingly, the silica particles and the PS particles can be differentiated by the first principal component (PC1), which accounts for 74.09% of the overall variance in the dataset. In addition, the PS particles of different sizes were clearly separated from each other, with the repeated measurements on the same particles clustered together. The 85-nm PS particles were separated from the two smaller particles by the second principal component (PC2). The two smaller PS particles located at the same corner on the scores plot but were still differentiable from each other: they both had hydrodynamic size around 45 nm but differed in their zeta-potentials. Similarly, the two silica particles experiencing longer amination process located closer to each other on the scores plot, while the one going through only 1 hr amination was farther away. Our results support that fluorescamine labeling can detect

protein-particle interaction and the interaction profile is strongly dependent on particle properties.

PCA also calculates the correlation of each variable with each principle component, and the result is displayed in the form of loading plot (Figure S3 in Supporting Information). The vectors of fibrinogen, HSA, thyroglobulin, and catalase all aligned with the axis of PC1 with minimal projection in the dimension of PC 2, indicating their important contribution in determination of PC1 that differentiated particles based on their core materials. Cyt C, transferrin and hemoglobin contributed more heavily to distribution along PC2, which differentiated the PS particles by their sizes. The nanoparticle fluorescence intensity, although small, also contributed to differentiation between the silica nanoparticles with longer amination times. The longer amination duration may have left more amines on the surface uncovered by carboxyl groups, yielding higher background fluorescence.

Fluorescamine assay for detection of protein interaction with non-transparent nanoparticles. Although the above on-plate screening method is rapid, it can only be applied to optically transparent nanoparticles. In order to use this method on non-transparent nanoparticles, separating the particles from the fluorescently-tagged proteins is required before signal acquisition. To achieve this, a filter-assisted enzymatic digestion was used to separate the resulting peptides from the nanomaterials. Due to the labeling of the lysine and arginine residues, chymotrypsin was chosen as the digestion protease. Tris was used to quench the remaining fluorescamine prior to digestion.

IONPs, possessing identical core diameters of 10 nm, were incubated with albumin, transferrin, or thyroglobulin before fluorescamine reaction and on-filter digestion. One of the

IONPs was coated with polyethylene glycol (abbreviated as PEG); and the other two were coated with an amphiphilic surface coating (AMP1 and AMP2). The two AMP-coated IONPs, produced by the manufacturer under identical synthetic conditions, possessed statistically similar sizes measured by DLS. However, their zeta potentials varied by 20 mV (Table 1). After digestion, the filtrate was collected for fluorescence analysis. PCA on the fluorescence profiles (Figure S4A, Supporting Information) showed excellent grouping result on the scores plot, with all three types IONPs well separated from each other (Figure 4). The first principal component, containing 75% of the total variance, is sufficient to separate the two AMP-coated IONPs from the PEG-coated IONPs, due to the difference of surface ligand material and the zeta-potential. The two different batches of AMP were separated by the 2nd principal component, which accounted for 25% of the overall variance, owing to their zeta-potential difference.

The loading plot (Figure S4A) shows that HSA and thyroglobulin were responsible for the differentiation between the PEG- and AMP-coated particles. Little change in the fluorescence of these two proteins was observed when bound to the PEG-coated particles, i.e. the normalized fluorescence close to 1 (Fig S4B). This could be due to the resistance of PEG to protein binding, which is often used to prevent non-specific adsorptions of proteins on surfaces. But binding of HSA and thyroglobulin to the AMP-coated particles significantly reduced the quantity of surface amines accessible for fluorescamine labeling: the normalized fluorescence was lower than 0.4. It is possible that the electrostatic repulsion between the acidic proteins and the negatively charged particles required larger interaction surface to stabilize the interaction.

Interestingly, the binding situations of transferrin to the IONPs were quite different than those observed for HSA and thyroglobulin. Interaction with the IONPs exposed more amines on transferrin to be labeled by fluorescamine, yielding normalized fluorescence values ranging from

120% to 170%. Significant binding of transferrin to the IONP particles was also observed in our previous study that screened the protein corona formed on IONP particles.[43] Since transferrin is an iron binding protein, we speculate that it may target the iron ion on the IONP surface. Conformational change may be necessary to expose the iron binding site, which also revealed more amines for fluorescamine labeling. Between the two AMP particles, higher increase in fluorescence occurred to transferrin when it interacted with AMP-2, the particle with a more negative zeta-potential, making transferrin the differentiation factor for the two AMP particles shown on the loading plot. This phenomenon agrees with what we observed in Fig. 2 between the sulfonated and carboxylated PS particles.

Since the on-plate screening and the on-filter digestion method utilized the normalized fluorescence against the protein-only control, their results should be directly comparable. To demonstrate this, we employed all the normalized fluorescence data obtained from the PS, silica, and IO particles in PCA. In agreement with previous PCA results, clear grouping of the particles made of different core materials was displayed on the scores plot (Figure S5). The larger, 85-nm PS particles were well separated from the two smaller PS particles, as were the PEG-modified IONP from the ones coated by AMP. However, the three types of silica particles were not differentiable, indicating their relatively high similarity among each other, compared to the difference among the PS particles or the IONPs.

Conclusions

Our study proves that fluorescamine labeling can be used to detect nanoparticle-protein interaction, because of its capability in targeting the surface amines on proteins. Formation of the binding interface would block some surface amines from being assessed by fluorescamine; on

the other hand, protein conformational changes could expose buried amines to be labeled. Distinct differences in fluorescence post-labeling can be observed before and after incubating the protein with nanoparticles. Although the exact reason for the fluorescence change can only be understood by investigations using other analytical tools, our results have demonstrated that the fluorescamine assay can serve as a rapid screening method for probing the interaction between a large number of proteins and nanoparticles. The obtained fluorescence profile can be used to study the relationship between particle property and protein interaction, as well as to determine batch similarity of the material prior to more expensive, low-throughput characterization. Such screening could be useful for initial assessment of the biological activity and safety of nanoparticles for biomedical applications.

The technique has limitations in that it is not readily suited for testing particles coated with amine groups, or proteins low in amine content like ConA and Cyt C, which will offer low signal changes compared to proteins with a higher degree of amine content. However, such difficulties could be solved if fluorogenic dyes targeting different functional groups (such as thiol or hydrophobic residues) on proteins are employed. In addition, for screening interactions on non-amine coated particles aiming to reveal changes in particle's physical parameters, suitable proteins with adequate amine contents can be chosen to ensure large signal changes can be observed.

Nevertheless, follow-up studies are needed for further exploration the applicability of our method, using proteins and particles with more diverse properties. For example, the method's efficacy on screening particle-protein interactions governed by hydrophobic forces is not clear, since the assay targets amine groups which are involved more in hydrophilic interactions. It will still be useful, if the binding results in partial unfolding of the protein to reveal the amine groups

originally buried inside the tertiary structure of the protein. More studies using proteins and particles with more diverse properties are needed in order to answer this question, which should not be difficult with the high-throughput sampling capability of our method. Once the binding situations are disclosed by fluorescamine labeling, more detailed studies with techniques that can reveal the exact degree and type of structural changes in proteins, like CD, can be performed on specific protein-particle pairs to obtain more insightful information about the interactions.

ASSOCIATED CONTENT

Supporting Information. Synthesis of carboxylated silica nanoparticles, FASP protocol, optimization of the fluorescamine assay method, CD measurement, table of proteins used in the on-plate assay, table of normalized fluorescence values used in PCA, additional denaturation tests, fluorescence profiles and loadings plots for differentiation based on different particle properties. This material is available free of charge via the Internet at http://pubs.acs.org

AUTHOR INFORMATION

Corresponding Author

[+]Email: wenwan.zhong@ucr.edu. Tel: +1-951-827-4925. Fax: +1-951-827-4713.

Author Contributions

The manuscript was written through contributions of all authors. All authors have given approval to the final version of the manuscript.

ACKNOWLEDGMENT

This work was supported by National Science Foundation CAREER Grant No. 1057113 for W. Zhong. J.Ashby was supported by the National Science Foundation Graduate Research Fellowship under Grant Number DGE-0813967. E. Ligans was supported by the California Alliance for Minority Participation (CAMP) at UCR. M. Tamsi was supported by the Kuwana - Sawyer undergraduate award of the Department of Chemistry, UCR. The authors are also very grateful for the UCR's Institute for Integrative Genome Biology for the usage of the Victor II plate reader.

REFERENCES

(1) Schulze, C.; Kroll, A.; Lehr, C. M.; Schafer, U. F.; Becker, K.; Schnekenburger, J.; Isfort, C. S.; Landsiedel, R.; Wohlleben, W. *Nanotoxicology***2008**, *2*. 51-U17;Mu, Q.; Jiang, G.; Chen, L.; Zhou, H.; Fourches, D.; Tropsha, A.; Yan, B. *Chemical Reviews (Washington, DC, United States)***2014**, *114*. 7740-7781;Nystroem, A. M.; Fadeel, B. *Journal of Controlled Release***2012**, *161*. 403-408;Rivera-Gil, P.; Jimenez De Aberasturi, D.; Wulf, V.; Pelaz, B.; Del Pino, P.; Zhao, Y.; De La Fuente, J. M.; Ruiz De Larramendi, I.; Rojo, T.; Liang, X.-J.; Parak, W. J. *Accounts of Chemical Research***2013**, *46*. 743-749.
(2) Gao, H.; He, Q. *Expert Opinion on Drug Delivery***2014**, *11*. 409-420.
(3) Mahmoudi, M.; Lynch, I.; Ejtehadi, M. R.; Monopoli, M. P.; Bombelli, F. B.; Laurent, S. *Chemical Reviews (Washington, DC, United States)***2011**, *111*. 5610-5637.
(4) Saptarshi, S. R.; Duschl, A.; Lopata, A. L. *Journal of Nanobiotechnology***2013**, *11*. 26;White, J. W.; Perriman, A. W.; McGillivray, D. J.; Lin, J.-M. *Nuclear Instruments & Methods in Physics Research, Section A: Accelerators, Spectrometers, Detectors, and Associated Equipment***2009**, *600*. 263-265;You, C.-C.; De, M.; Rotello, V. M. *Current Opinion in Chemical Biology***2005**, *9*. 639-646.
(5) Chithrani, B. D.; Ghazani, A. A.; Chan, W. C. W. *Nano Letters***2006**, *6*. 662-668.
(6) Gagner, J. E.; Qian, X.; Lopez, M. M.; Dordick, J. S.; Siegel, R. W. *Biomaterials***2012**, *33*. 8503-8516.
(7) Walkey, C. D.; Olsen, J. B.; Guo, H. B.; Emili, A.; Chan, W. C. W. *Journal of the American Chemical Society***2012**, *134*. 2139-2147.
(8) Ashby, J.; Schachermeyer, S.; Pan, S.; Zhong, W. *Analytical Chemistry (Washington, DC, United States)***2013**, *85*. 7494-7501;Li, N.; Zeng, S.; He, L.; Zhong, W. *Analytical Chemistry (Washington, DC, United States)***2010**, *82*. 7460-7466.
(9) Piehler, J. *Current Opinion in Structural Biology***2014**, *24*. 54-62;Li, L.; Mu, Q.; Zhang, B.; Yan, B. *Analyst (Cambridge, United Kingdom)***2010**, *135*. 1519-1530.
(10) Zhang, H.; Burnum, K. E.; Luna, M. L.; Petritis, B. O.; Kim, J.-S.; Qian, W.-J.; Moore, R. J.; Heredia-Langner, A.; Webb-Robertson, B.-J. M.; Thrall, B. D.; Camp, D. G.; Smith, R. D.; Pounds, J. G.; Liu, T. *Proteomics***2011**, *11*. 4569-4577.
(11) Pan, H.; Qin, M.; Meng, W.; Cao, Y.; Wang, W. *Langmuir***2012**, *28*. 12779-12787.
(12) Tenzer, S.; Docter, D.; Rosfa, S.; Wlodarski, A.; Kuharev, J.; Rekik, A.; Knauer, S. K.; Bantz, C.; Nawroth, T.; Bier, C.; Sirirattanapan, J.; Mann, W.; Treuel, L.; Zellner, R.; Maskos, M.; Schild, H.; Stauber, R. H. *ACS Nano***2011**, *5*. 7155-7167;Bar-Ilan, O.; Albrecht, R. M.; Fako, V. E.; Furgeson, D. Y. *Small***2009**, *5*. 1897-1910.
(13) Moghimi, S. M.; Muir, I. S.; Illum, L.; Davis, S. S.; Kolbbachofen, V. *Biochimica Et Biophysica Acta***1993**, *1179*. 157-165;Lundqvist, M.; Stigler, J.; Elia, G.; Lynch, I.; Cedervall, T.; Dawson, K. A. *Proc. Natl. Acad. Sci. U. S. A.***2008**, *105*. 14265-14270;Gref, R.; Luck, M.; Quellec, P.; Marchand, M.; Dellacherie, E.; Harnisch, S.; Blunk, T.; Muller, R. H. *Colloid Surf. B-Biointerfaces***2000**, *18*. 301-313;Natte, K.; Friedrich, J. F.; Wohlrab, S.; Lutzki, J.; von Klitzing, R.; Osterle, W.; Orts-Gil, G. *Colloid Surf. B-Biointerfaces***2013**, *104*. 213-220.
(14) Asharani, P. V.; Yi, L. W.; Gong, Z. Y.; Valiyaveettil, S. *Nanotoxicology***2011**, *5*. 43-54;Casals, E.; Pfaller, T.; Duschl, A.; Oostingh, G. J.; Puntes, V. F. *Small***2011**, *7*. 3479-3486.
(15) Kelly, S. M.; Jess, T. J.; Price, N. C. *Biochimica et Biophysica Acta (BBA) - Proteins and Proteomics***2005**, *1751*. 119-139;Wang, L. M.; Li, J. Y.; Pan, J.; Jiang, X. M.; Ji, Y. L.; Li, Y. F.; Qu, Y.; Zhao, Y. L.; Wu, X. C.; Chen, C. Y. *Journal of the American Chemical Society***2013**, *135*.

17359-17368;Billsten, P.; Wahlgren, M.; Arnebrant, T.; McGuire, J.; Elwing, H. *Journal of Colloid and Interface Science***1995**, *175*. 77-82;Venyaminov, S. Y.; Vassilenko, K. S. *Analytical Biochemistry***1994**, *222*. 176-184;Venyaminov, S. Y.; Klimtchuk, E. S.; Bajzer, Z.; Craig, T. A. *Analytical Biochemistry***2004**, *334*. 97-105.
(16) Vertegel, A. A.; Siegel, R. W.; Dordick, J. S. *Langmuir***2004**, *20*. 6800-6807.
(17) Jans, H.; Liu, X.; Austin, L.; Maes, G.; Huo, Q. *Anal. Chem.***2009**, *81*. 9425-9432;James, A. E.; Driskell, J. D. *Analyst***2013**, *138*. 1212-1218.
(18) Udenfrie.S; Stein, S.; Bohlen, P.; Dairman, W. *Science***1972**, *178*. 871-&.
(19) Noble, J. E.; Knight, A. E.; Reason, A. J.; Di Matola, A.; Bailey, M. J. A. *Mol. Biotechnol.***2007**, *37*. 99-111;Joo, W.-A.; Speicher, D. W. *Current protocols in protein science / editorial board, John E. Coligan ... [et al.]***2007**, *Chapter 10*. Unit 10.6.
(20) Birlouez-Aragon, I.; Leclere, J.; Quedraogo, C. L.; Birlouez, E.; Grongnet, J. F. *Nahr.-Food***2001**, *45*. 201-205;Chen, Y.; Zhang, Y. Q. *Anal. Bioanal. Chem.***2011**, *399*. 2503-2509;Dhaunta, N.; Fatima, U.; Guptasarma, P. *Analytical Biochemistry***2011**, *408*. 263-268.
(21) Stockert, J. C.; Blazquez, A.; Galaz, S.; Juarranz, A. *Acta Histochem.***2008**, *110*. 333-340.
(22) Raussens, V.; Ruysschaert, J.-M.; Goormaghtigh, E. *Analytical Biochemistry***2003**, *319*. 114-121.
(23) Wisniewski, J. R.; Zougman, A.; Nagaraj, N.; Mann, M. *Nature Methods***2009**, *6*. 359-U60.
(24) An, Y. Q.; Chen, M.; Xue, Q. J.; Liu, W. M. *Journal of Colloid and Interface Science***2007**, *311*. 507-513.
(25) Ashby, J.; Pan, S.; Zhong, W. *ACS Applied Materials and Interfaces***2014**, *6*. 15412–15419.
(26) Schachermeyer, S.; Ashby, J.; Kwon, M.; Zhong, W. W. *J. Chromatogr. A***2012**, *1264*. 72-79.
(27) Fraczkiewicz, R.; Braun, W. *Journal of Computational Chemistry***1998**, *19*. 319-333.

(28) "TANAGRA: a free software for research and academic purposes", *Proceedings of EGC (in French)*, 2005, RNTI-E-3.697-702.

Table and figure captions:

Table 1. Physical parameters of nanoparticles investigated as part of the study, as well as their abbreviations in PCA analysis.

Table 2. Comparison of the total number of lysine/arginines, theoretically determined number of surface accessible lysines and arginines, and experimentally calculated number of fluorescamine binding events for five model proteins.

Figure 1. Fluorescamine fluorescence intensities of proteins incubated in either buffer or 50% ethanol to demonstrate increased fluorescamine activity on denatured proteins. Fluorescence intensities shown are less the fluorescence of a buffer blank.

Figure 2. Normalized fluorescence changes of proteins after incubation with either A) polystyrene or B) silica nanoparticles. Fluorescence intensities were normalized to the buffer-only protein fluorescence.

Figure 3. PCA scores plot showing the ability of the fluorescamine assay to differentiate between six different particles of varying physiochemical parameters.

Figure 4. PCA scores plot showing differentiation between iron oxide nanoparticles with differing surface coatings. Circles – AMP-1, diamonds – AMP-2, triangles – PEG.

Table 1.

Particle	Abbrev. in PCA	Average Hydrodyn. Diameter	Average Zeta Potential
42 nm carboxylated polystyrene (PS)	PS-1	42 ± 6 nm	-45 mV
48 nm carboxylated polystyrene	PS-2	48 ± 7 nm	-87 mV
85 nm carboxylated polystyrene	PS-3	85 ± 7 nm	-67 mV
Silica (Si) particle aminated for 1 hr before carboxylation	Si-1	87 ± 18 nm	-44 mV
Silica particle aminated for 4 hrs before carboxylation	Si-2	94 ± 16 nm	-42 mV
Silica particle aminated for 24 hrs before carboxylation	Si-3	84 ± 12 nm	-51 mV
10nm IONP with an amphiphilic (AMP) polymer coating	AMP-1	15 ± 5 nm	-48 mV
10nm IONP with an amphiphilic polymer coating	AMP-2	13 ± 3 nm	-62 mV
10nm IONP with a polyethylene (PEG) glycol coating	PEG	27 ± 6 nm	-17 mV

Table 2.

Protein	Total Lys/Arg	Surface Lys/Arg (GETAREA)	Binding events (Fluorescamine)
Alpha-1-Antitrypsin	41	28	29.8 ± 0.9
Apolipoprotein A1	37	13	16.4 ± 5.0
Haptoglobin	44	25	24.2 ± 4.4
Serum Albumin	83	37	38.9 ± 1.4
Transferrin	84	34	46.4 ± 2.8

Figure 1.

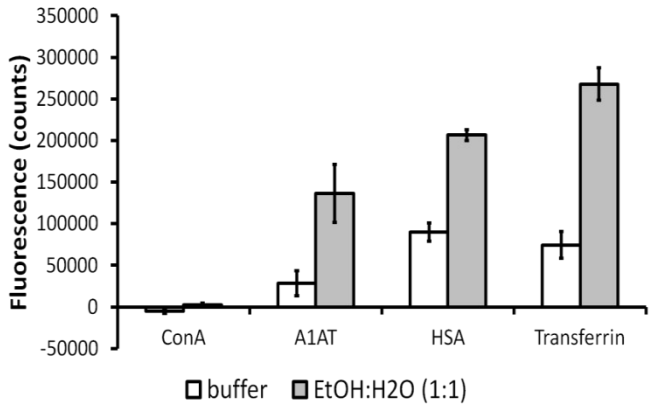
350000
300000
250000
200000
150000
100000
50000
0
-50000
Fluorescence (counts)
ConA
A1AT
HSA
Transferrin
buffer
EtOH:H2O (1:1)

Figure 2.
A)

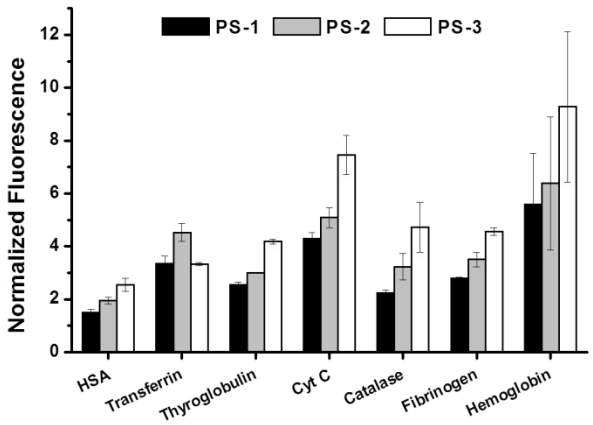
PS-1
PS-2
PS-3
Normalized Fluorescence
0
2
4
6
8
10
12
HSA
Transferrin
Thyroglobulin
Cyt C
Catalase
Fibrinogen
Hemoglobin

B)

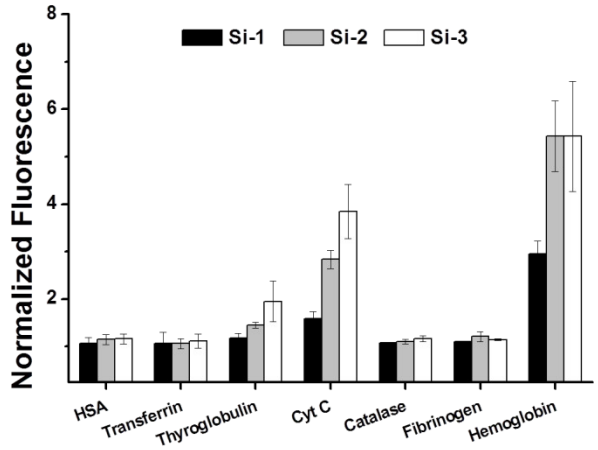
Si-1
Si-2
Si-3
Normalized Fluorescence
2
4
6
8
HSA
Transferrin
Thyroglobulin
Cyt C
Catalase
Fibrinogen
Hemoglobin

Figure 3.

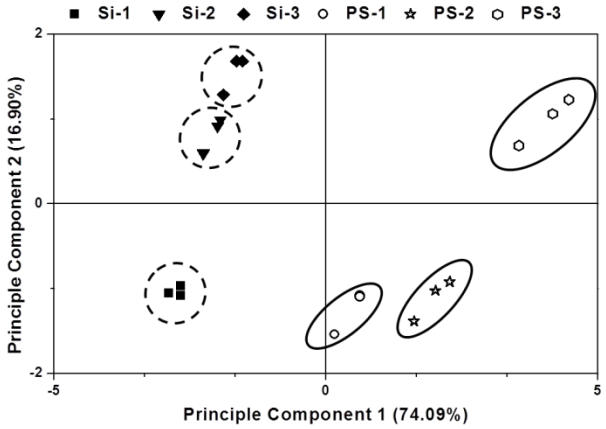
Si-1
Si-2
Si-3
PS-1
PS-2
PS-3
Principle Component 2 (16.90%)
Principle Component 1 (74.09%)
2
0
-2
-5
0
5

Figure 4.

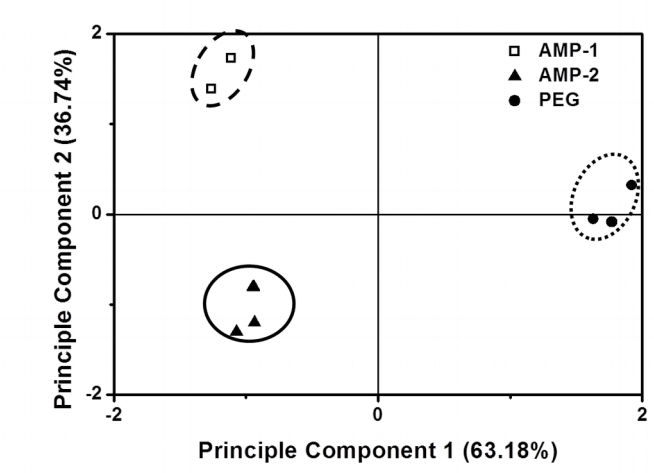
AMP-1
AMP-2
PEG
Principle Component 2 (36.74%)
Principle Component 1 (63.18%)
2
0
-2
-2
0
2

Table of Contents (TOC) Figure: